Biosensors and Bioelectronics 26 (2010) 149–154

Contents lists available at ScienceDirect

Biosensors and Bioelectronics

journal homepage: www.elsevier.com/locate/bios

Multi-targeting single fiber-optic biosensor based on evanescent wave and quantum dots

Youlin Zhang[a,b], Qinghui Zeng[a], Yajuan Sun[a], Xiaomin Liu[a], Langping Tu[a], Xianggui Kong[a,*], Wybren Jan Buma[b], Hong Zhang[b,**]

[a] Key Laboratory of Excited State Processes, Changchun Institute of Optics, Fine Mechanics and Physics, Chinese Academy of Sciences, 3888 Eastern South Lake Road, Changchun 130033, China
[b] Van't Hoff Institute for Molecular Sciences, University of Amsterdam, Nieuwe Achtergracht 166, 1018 WV Amsterdam, The Netherlands

ARTICLE INFO

Article history:
Received 12 March 2010
Received in revised form 27 April 2010
Accepted 25 May 2010
Available online 2 June 2010

Keywords:
Fiber-optic evanescent wave biosensor
Multiplexed immunoassay
Quantum dots
CdSe/ZnS
Affinity

ABSTRACT

Highly sensitive, multi-analyte assay is a long-standing challenge for a single fiber-optic evanescent wave biosensor (FOB). In this paper, we report the first realization of such kind of FOB using CdSe/ZnS core/shell quantum dots (QDs) as labels. A direct binding assay model between antibody and antigen was employed to demonstrate the advantages of using QDs, instead of conventional fluorescein isothiocyanate (FITC), in lifting the sensitivity. Especially, multiplexed immunoassay was demonstrated in a single fiber FOB constructed with four differently sized QDs. Furthermore, the phenomenon that the affinity of the QD-labeled human IgG (QD-IgG) with goat anti-human IgG (anti-IgG) was lower than that of the FITC-labeled human IgG (FITC-IgG) was investigated and was ascribed to the differences in size and mass of the two. Our study indicates that the affinity could be improved by controlling the amount of IgG binding on QDs.

1. Introduction

Fiber-optic evanescent wave biosensor (FOB) has been a subject of intensive research in the past decades. FOB is based on molecular recognition and evanescent wave sensing to detect various analytes, where excitation light propagating through the fiber excites fluorophores within a certain distance (~hundreds of nm) of the fiber core surface (Leung et al., 2007; Taitt et al., 2005). Thus, the system is highly selective for the surface-bound fluorophores in contrast to cuvette-based measurements where the signal from the unbound labeled antigen may dominate. Because of their efficiency, accuracy, low cost, and convenience, FOB is a promising alternative to traditional immunological methods for biomolecule measurements. Under development of last thirty years, some FOBs (e.g. Analyte 2000 and RAPTOR, two commercial products) have been applied into medical pathogens, food toxicity, biochemical weapons, fast detection for environmental samples, etc. At present, methods to increase FOB sensitivity and multi-analyte detection capabilities are the focus of attention. The RAPTOR can simultaneously detect four different target analytes by dexterously designing a microfluidics system. The microfluidics can be incorporated for parallel sample analyses, improving assay speed, and enhancing sensitivity. However, the multi-targeting is performed by a multi-fiber system and each fiber is still single targeting, which limits further expanding of the multi-targeting assay capabilities. In fact, realization of multi-analyte assay capabilities in a single fiber of FOB is hindered because the used labels are organic fluorophores which have inherent drawbacks, such as narrow excitation bands, broad emission bands, and a low resistance to photodegradation (Taitt et al., 2005; King et al., 1999). Therefore, looking for the good fluorescent tag is and will be an ongoing major goal in this field.

Quantum dots (QDs) are inorganic fluorophores that have the potential to circumvent these limitations encountered by organic fluorophores. In particular, CdSe/ZnS core–shell QDs exhibit a high resistance to photodegradation, and size-dependent, tunable and high-yield photoluminescence (PL). These unique features make QDs quickly a promising candidate, to replace the organic fluorophores, in biological applications. These applications include, amongst others, *in vivo* animal targeting, *in vivo* live cell imaging, cytology, and bioanalytical assays and biosensors (Michalet et al., 2005; Alivisatos, 2004; Pinaud et al., 2004; Yuan et al., 2008). Moreover, the absorption spectra of QDs are broad, whereas the emission bands are narrow and symmetrical, and occur in the visible spectral range (Dayal and Burda, 2007; Zhao et al., 2007). Simultaneous determination of multiplex analytes is thus expected by multi-color QDs, which has been proved in other detection techniques (Goldman et al., 2004; Peng et al., 2009). Although it was predicted

* Corresponding author. Tel.: +86 431 86176313.
** Corresponding author. Tel.: +31 20 5256976.
E-mail addresses: xgkong14@ciomp.ac.cn (X. Kong), h.zhang@uva.nl (H. Zhang).

0956-5663/$ – see front matter © 2010 Elsevier B.V. All rights reserved.
doi:10.1016/j.bios.2010.05.032

that the use of quantum dots as labels would be an increasing focus for FOB research and development (Taitt et al., 2005), up to now, no report has appeared on the application of QDs in FOB.

On the other hand, compared with organic fluorophores, the size and mass of a QD are much larger than a single dye molecule and compatible to simultaneous conjugate with more than one biomolecule. This substantial increase in molecular mass results in reduced diffusion coefficient for the protein in solution (Jaiswal and Simon, 2004). Added QDs also restrict the rotational motion of the conjugated protein in solution, reducing the probability that the protein finds the correct orientation for binding. The implication of reduced freedom of motion manifests in potential changes to the equilibrium binding rate constants and overall protein to protein affinity (Swift and Cramb, 2008). On top of the function of assay, FOB can also acquire the binding kinetics, such as the association and dissociation rate constants. Thus the influence of QDs on the affinity between protein molecules can also be evaluated by FOB.

In this work, we were successful in tailored constructing a multi-targeting single fiber of FOB, which combined FOB with CdSe/ZnS core/shell QDs as labels. The detection limit and affinities of the QD-based FOB were compared with those of conventional FITC FOB. It was proposed and proved also that the affinity between anti-IgG and QD-labeled IgG (QD-IgG) could be enhanced by controlling the amount of IgG on the conjugates of QD-IgG. To demonstrate its multi-targeting function, four-analyte immunoassays were carried out by using four sizes of QDs bounded on the surface of a single fiber.

2. Materials and methods

2.1. Reagents and chemicals

All solvents and chemicals used in this study were of analytical or chemical pure grade. FITC-labeled human IgG (FITC-IgG) was purchased from Dingguo Biotechnology Development (China). All other materials were purchased from Sigma–Aldrich.

2.2. Equipment

The detection scheme of the FOB (Fig. S1) was described in our previous report (Chao et al., 2005). Briefly, a laser beam of 488 nm line of a Spectra-Physics Model 164 Argon ion laser was guided into an optical fiber through an objective lens (20×, NA = 0.5) to match the numerical aperture of the fiber (NA = 0.47). A multimode silica fiber of 800 μm in core diameter was adopted. The reaction chamber (500 μL in volume) was modified from a plastic cuvette for loading solution. The fluorescence signal was generated by exciting the fluorophore labeled on biomolecules, filtered with a band pass filter (±10 nm at 488 nm) to reduce the background noise, and finally detected by a Peltier air-cooled CCD.

2.3. Preparation of aldehyde-functionalized fiber probe

Plastic clad, silica optical fibers (800 μm core) fitted with plastic ferrule were stripped of their cladding at the proximal end and buffered 12.5 cm from their distal end. The exposed core was cleaned with a concentrated hydrochloric acid:methanol (1:1) solution for 30 min, followed by concentrated sulfuric acid for 30 min. The fibers were then boiled in water for 20 min, dried in 60 °C oven full of nitrogen, and coated with a 10% (v/v) solution of aminopropyltriethoxysilane in acetone. The amine-terminated surface of the silica fiber was modified by reacting with 5% solution of glutaraldehyde (Cho) in phosphate-buffered saline (PBS) of pH 7.4 for 1 h. Subsequently, the fiber was rinsed with deionized water and dried in a stream of nitrogen.

2.4. Synthesis of water-soluble CdSe/ZnS QD

Organic-soluble CdSe/ZnS core–shell QDs (Hines et al., 1996; Shan et al., 2005) emitting at 650 nm were precipitated from the initial butanol stock solution with methanol, rinsed with methanol, and dried under vacuum. QDs were redispersed in a 5 mg/mL octylamine-modified polyacrylic acid solution in chloroform. The molar ratio of polyacrylic acid and QDs was kept above 500:1. The tube containing the mixture of polymer and QDs was evaporated. The residue was dissolved in water, and purified from excess polymer by gel filtration. The purified solution of QDs coated with polymer could then be stored in 10 mM borate buffer, pH 8.2 in the dark for at least 2 months without any aggregate or precipitate formation. Poly (ethylene glycol) derivatives were grafted on the surface of QDs coated with polymer. QDs were functionalized with amine groups by coupling with PEG-5000-amine (Wu et al., 2003; Feng et al., 2005). The QDs with emission maxima at 650 nm were ellipsoid with a core/shell diameter of 6 nm (minor axis) × 12 nm (major axis) (see Fig. S2A). The hydrophilic coatings enlarged the size of the QDs several-fold in aqueous solution as a result of solvation effects, reflected in an increase of the hydrodynamic diameter (∼24 nm). The structure of water-soluble QDs with the capping ligand TOPO and an encapsulating polymer layer is shown in Fig. S2B. The QDs emitting at 525, 565 and 605 nm were also prepared using the same method and their hydrodynamic diameters are 15 nm, 19 nm and 21 nm, respectively.

2.5. Preparation of QD-human IgG (QD-IgG) conjugates

The 2 nmol amine-QDs were reacted with Cho in a ratio of 1 to 500 for 5 h. In order to remove the excess Cho molecules, the resulting samples were centrifuged in Microcon Centrifugal Filter Devices (50,000 Nominal Molecule Weight Limit). The functionalized QDs were then coupled with human IgG (IgG) to produce QD-human IgG conjugates (QD-IgG), where the amount of IgG was 2–80 nmol. Afterwards, the product was purified by Sephadex-150 filtration column chromatography. The conjugation of IgG and QDs was confirmed by the agarose gel (0.8%) electrophoresis technique. Preparation of QD-human fibrinogen (QD-Fib) and QD-human serum albumin (QD-HSA) conjugates was also completed using the above method.

2.6. Determination of IgG/QD ratios

FITC-IgG was used as a trail in the coupling procedure in order to evaluate the number of IgG molecules bound per QD (Goldman et al., 2002). IgG was labeled with 7 molecules of FITC according to the manufacturer's instructions. The QD-IgG was then prepared using FITC-IgG followed by removal of unbound antibody as described above. The number of IgG per QD was calculated using the FITC absorbance at 490 nm of the purifier product. The QD absorption at 490 nm was deducted.

2.7. Immunoassays

The aldehyde-functionalized fiber probes were coated overnight (4 °C) with serial dilutions of anti-IgG dissolved in PBS buffer (pH 7.4). The concentration of anti-IgG was set respectively as 1, 5, 10, 50, 250, 500, 700 and 1000 ng/mL. In the control experiments, the aldehyde-functionalized fiber only reacted with the same volume of buffer containing no anti-IgG for nonspecific binding. After removing excess anti-IgG or blank solutions from the reaction chamber, the probes were blocked at 4 °C for 2 h with PBS containing 2% (w/v) BSA. The probes were then washed 3 times with PBST (PBS with 0.1% Tween 20), and QD- or FITC-IgG were placed into the chamber to test and control probes and incu-

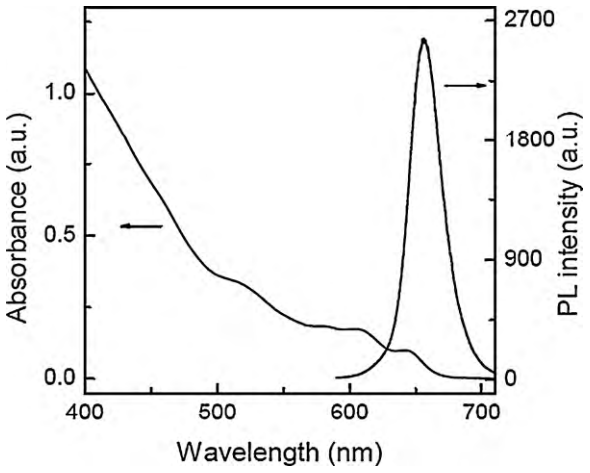

Fig. 1. Absorption and photoluminescence (PL) spectra of water-soluble polymer-capped CdSe/ZnS QDs. The excitation wavelength is 488 nm.

bated for 15 min. Unbound QD-IgG was removed and discarded. The probes were then washed three times with PBS, followed by fluorescence measurement. The obtained anti-IgG/QD- or FITC-IgG complex was able to emit fluorescence on excitation by the evanescent wave near the uncladded fiber surface. Because the penetration depth of the fiber-mediated evanescent wave in solution was approximately 200 nm from the uncladded fiber surface, only QD- or FITC-conjugated antigen bounded with antibody in conjunction with fiber-immobilized capture antibody could be excited. To obtain the binding curves, the time response of anti-IgG/FITC- or QD-IgG interaction was measured by recording the fluorescence signals. For the multiplexed assays, the aldehyde-functionalized fiber probes were coated overnight (4 °C) with serial dilutions of anti-Fib, anti-HAS, Hepatitis B surface antibody (anti-HBs) and anti-IgG dissolved in PBS buffer (pH 7.4).

3. Results and discussion

Spectral properties of water-soluble polymer-capped CdSe/ZnS QDs are presented in Fig. 1, where the characteristic and narrow excitonic absorption peak is at 645 nm and the luminescence is peaked at 655 nm with a full width at half maximum (FWHM) of 25 nm when excited at 488 nm. The emission quantum yield was 35% as determined using Rhodamine 6G (95%). Compared with oil-soluble QDs (53% of quantum yield), no changes appeared in the peak positions, shapes and FWHM of the absorption and PL spectra, indicating that the phase transfer did not alter the optical properties of QDs.

The polymer-capped QDs had the functional amino group, which could be conjugated with the amino group of human IgG by Cho. During conjugation, Cho, acting as a crossing reagent, was used to facilitate the coupling of human IgG onto the surface of QDs. To confirm the binding of QDs to human IgG, agarose gel electrophoresis was performed. The agarose gel luminescence image (excitation at 360 nm) is shown in Fig. 2A. Because the QDs held positive charges, the QDs moved to the negative electrode (Fig. 2A, well 1) in the electric field. When Cho was coupled to the QDs, amine groups on the QD surface disappeared, resulting in the neutralization of the surface charge of QDs, thus limiting the mobility of Cho-QDs and the traveling distance (Fig. 2A, wells 2, 3, 6 and 7). After coupling human IgG onto the surface of the QDs, the conjugates of QD-IgG became negatively charged. This caused QD-IgG move to the anode (Fig. 2A, wells 4, 5, 8 and 9). All these results verified that the QDs were indeed conjugated to human IgG. To investigate the effect of the coupling processes on the PL properties of the QDs, the spectra were recorded against different conjugates (Fig. 2B). Regarding the PL intensity, it is from high to low as the order of QD-IgG, QDs and Cho-QDs. This finding is in line with the previous argument that the Cho coupling process might destroy the surface of QDs, whereas protein could improve the PL (Mattoussi et al., 2000; Mamedova et al., 2001).

In our experiments, the QDs were used to replace FITC to label antigens to improve the performance of the FOB. We started with the comparison of the PL properties of the two complexes. Fig. 3A shows the PL spectra of water-soluble CdSe/ZnS QD-IgG in a PBS buffer with different concentrations of FITC-IgG. For the FITC-IgG, there were seven FITC molecules in an IgG molecule. However, even in this case, the fluorescent intensity of QD-IgG was still much higher (~3.6 times) than that of FITC-IgG as shown in Fig. 3A. The peak emission intensity of QDs was 3.6 times higher than that of FITC. It can therefore be expected that the sensitivity of the FOB using QDs could be increased with the same order.

Another factor influencing the sensitivity and stability of a sensor is the photostability of fluorophores. To compare the photostability of the QDs with FITC, the time dependent emission spectra of the QDs and the FITC were recorded at 180 s interval, under continuous excitation (see Fig. 3B). For clearly expressing the excellence of QDs over FITC, the ratio of FITC-IgG to QD-IgG was set as 5. Progressive enhancement of the PL intensity of the QDs was observed, whereas the position of PL peak remained unchanged. The enhancement should not be surprised since passivation should

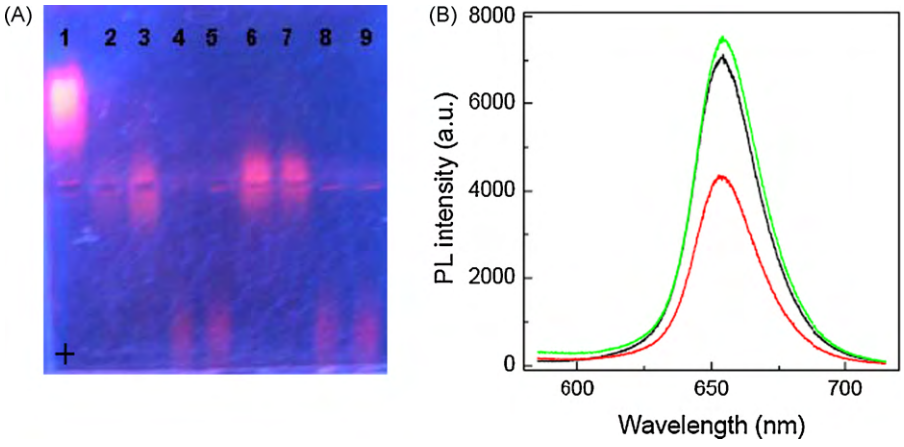

Fig. 2. (A) 0.8% agarose gel electrophoresis luminescent image of QDs, QD-Cho, and QD-IgG (excitation at 360 nm). Wells: 1-QDs; 2, 3, 6 and 7-QD-Cho; 4, 5, 8 and 9-QD-IgG. (B) The PL spectra of different conjugates of QDs (black line), QD-Cho (red line) and QD-IgG (green line). (For interpretation of the references to color in this figure legend, the reader is referred to the web version of the article.)

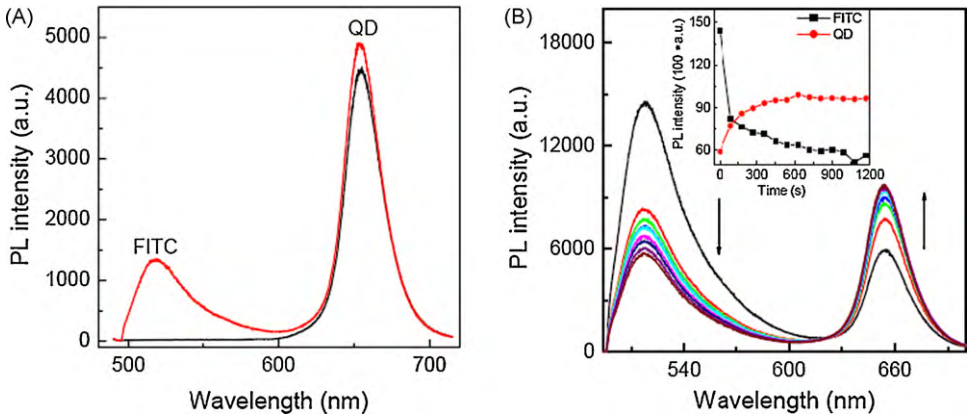

Fig. 3. (A) PL spectra of water-soluble CdSe/ZnS QD-IgG (IgG/QD ratio ≈1) in PBS buffer with different concentrations of FITC-IgG (the black line: FITC-IgG/QD-IgG ratio = 0; the red line: FITC-IgG/QD-IgG = 1). (B) Photo-stability of QDs compared with that of FITC-IgG. The arrows represent the direction of time increase (the time interval is 180 s). Inset: PL intensity of FITC-IgG and QD-IgG as a function of time. The concentration of QDs is 8.4×10^{-9} mol/L and the excitation wavelength is 488 nm; the FITC-IgG to QD-IgG ratio is 5. (For interpretation of the references to color in this figure legend, the reader is referred to the web version of the article.)

occur on the QD surface states that were not blocked by the capping agents (Myung et al., 2003). As for the FITC, the PL intensity decreased rapidly up to 180 s, and slowly afterwards. Although at the starting point, the PL intensity of FITC was higher than that of QDs when the ratio of FITC-IgG/QD-IgG was set as 5, at the end the PL intensity of QDs was higher, suggesting also that the sensitivity of the FOB should be increased when using QDs to replace FITC. A set of experiments was then designed on this issue.

The direct binding immunoassay model based on the binding of the QD-IgG with anti-IgG is illustrated in Fig. S3 (Anderson et al., 1997). The FITC-IgG interaction was characterized with anti-IgG at various concentrations and the detection limit was determined to be 10 ng/mL as reported previously (Chao et al., 2005). Direct binding assessment proved that the QD-IgG was able to bind to anti-IgG immobilized at the surface of the fiber core (Fig. 4A). Effects on fluorescent signals by varying the amount of anti-IgG were investigated using the QD-IgG as bioprobe. In these experiments, luminescence signal of the bound conjugate was measured over a range of anti-IgG concentrations from 1 ng/mL to 1 μg/mL. The signal increased linearly with anti-IgG concentrations until saturation was reached at 700 ng/mL. The calculated coefficient of correlation (R^2) was 0.998 from 5 ng/mL to 500 ng/mL, indicating a reasonable linear dynamic range. To prove the selectivity of the method, the fluorescence change of FOB upon addition of other proteins is shown in Fig. S4. Fig. S4 indicates the FOB holds a highly selective fluorescence response toward anti-IgG.

The FOB was not only used for *in vitro* detection as described above but also offered a powerful tool for monitoring protein interaction processes *in situ* and in real time, and thus could provide information on protein interaction kinetics and identify specific biomolecules in biomedical applications (Abel et al., 1996; Muller et al., 1997; Wang and Jin, 2003). To show the real-time analysis with the immunosensor, a fiber probe with anti-IgG was prepared and placed in the reaction chamber. The QD-IgG or FITC-IgG conjugate was poured into the cell. The binding processes between QD-IgG in solution and anti-IgG immobilized on the fiber surface were monitored by the FOB. The PL intensity was plotted versus time to get the binding curves. In order to measure the background noise of the sensor and validate the specificity of the QD-IgG, the control probe was added to the reaction chamber with QD-IgG for recording (Fig. 4B). Fig. 4B shows the control signal is very low, and almost changeless as time prolongs, which indicates the IgG retained its high specificity after the conjugation and furthermore proved that the proteins maintained their biological activities after conjugation to the QDs. The detection limit was calculated, following the IUPAC criterion, as the concentration of anti-IgG which produced an analytical signal three times the standard deviation of the control (or blank) signal and the calculated detection limit was of 5 ng/mL. Such a detection limit was lower to the most sensitive method reported for the anti-IgG detection (Wadkins et al., 1995; Wang et al., 2009). The reproducibility of the method was also evaluated. The relative standard deviation for six repeated measurements of

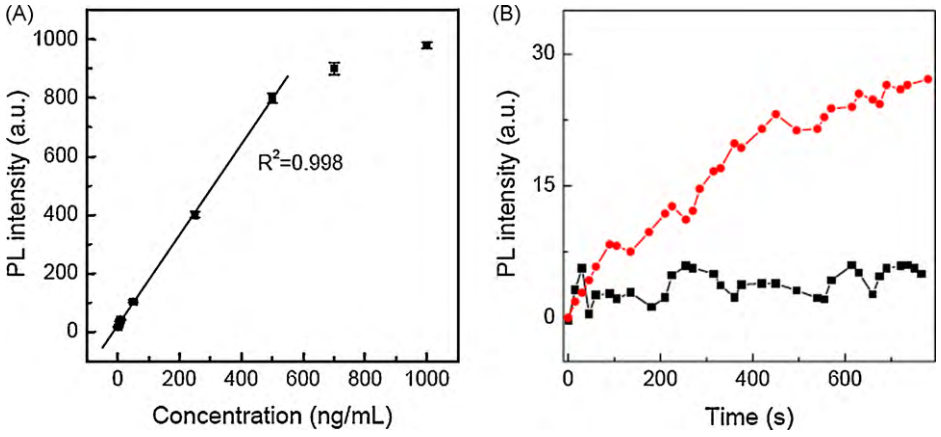

Fig. 4. (A) Direct binding detection of anti-IgG by QD-IgG (IgG/QD ratio ≈1) conjugates. Fiber core coated with varying concentrations of anti-IgG (ng/mL). (B) Binding curves of anti-IgG/IgG obtained by the immunosensor (square, 2 mg/mL nonspecific BSA; circle, 5 ng/mL anti-IgG).

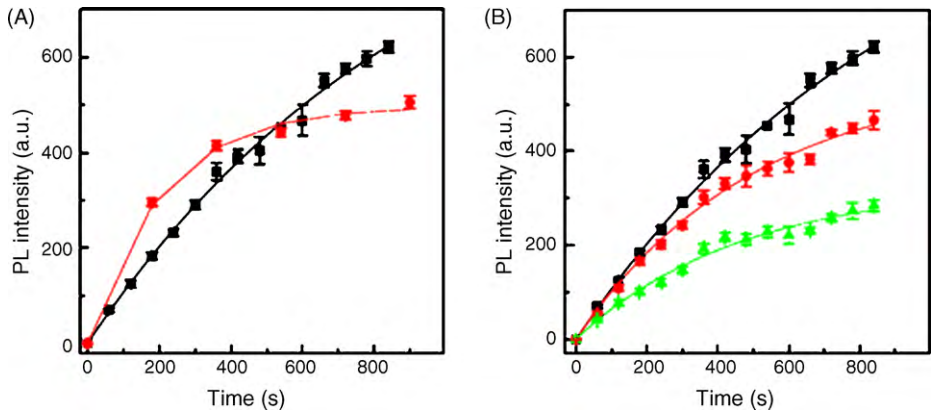

Fig. 5. (A) Binding curves between anti-IgG and QD- (square) or FITC-IgG (circle) obtained by the sensor at the same conditions. (B) Binding curves between anti-IgG and QD-IgG with different IgG to QD ratio (square: IgG/QD ≈ 1; circle: IgG/QD ≈ 3; triangle: IgG/QD ≈ 7). The concentration of QDs is constant in the experiment.

500 ng/mL anti-IgG was 2%. As mentioned above, the detection limit using FITC as a label was 10 ng/mL. Considering further the PL qualities of using QD and FITC in Fig. 3A, the sensitivity when using QDs should be significantly improved—much higher than 3.6 times than that using FITC because what detected here was peak emission intensities of labeled fluorophores in the FOB system. In our experiments, however, the sensitivity of FOB with QDs as label was only enhanced once.

Compared with FITC, the QDs have superior emission intensity and photostability. At the same time, the size and mass of QDs are much larger than a single dye molecule. This substantial increase in mass will affect the equilibrium binding rate constants and overall affinity of the protein for protein, which drawback may be responsible for the fact that the sensitivity of FOB with QDs was only enhanced once. Fig. 5A gives the binding curves of anti-IgG/FITC- or QD-IgG. Since the reaction between immobilized antibodies and antigens in solution can be assumed to follow pseudo-first-order kinetics (O'Shannessy et al., 1993), and the association rate constants or dissociation rate constants can be obtained by an analogous analysis method. In the data analytical process, the dissociation rate constants were set to the same values and the fitted curves are shown in Fig. 5. The association rate constants so obtained for anti-IgG/FITC- and QD-IgG are $1.38 \times 10^6\ M^{-1}\ s^{-1}$ and $0.17 \times 10^6\ M^{-1}\ s^{-1}$, respectively, which clearly indicated that the affinity of the FITC-IgG to the anti-IgG was better than that of the QD-IgG. It is well known that the size and mass of each QD, which are much larger than that of a single dye molecule, are compatible with a protein molecule. Thus the increased size and mass could interfere with the biomolecular mobility, and the affinity dropping down might be the consequence. To further study this issue, let us turn to the binding curves of anti-IgG/QD-IgG shown in Fig. 5B. Here, the amount of protein connected to the QDs was controlled in order to change the size and mass of the conjugates between protein and the QD. Following aforementioned methods, the calculated association rate constants, in the order of increasing the IgG to QD rate, are $1.70 \times 10^5\ M^{-1}\ s^{-1}$, $1.38 \times 10^5\ M^{-1}\ s^{-1}$, and $0.70 \times 10^5\ M^{-1}\ s^{-1}$, respectively, i.e. increasing the size and mass of the conjugates reduced the affinities of anti-IgG/QD-IgG. Thus, it is confirmed that the much bigger size and mass of the QDs, compared to the FITC molecules, interfered with the biomolecular mobility and reduced the affinities of the QD-IgG. On the other hand, a crossing point between the two binding curves appears in Fig. 5A. The binding reaction between FITC-IgG and anti-IgG approaches saturation in about 10 min, whereas the binding curve between QD-IgG and anti-IgG increases all along as time prolongs until the binding reaction saturates in about 30 min—increasing of detecting time can improve the sensitivity of FOB. In the mean time, Fig. 5B indicates also that the affinity can be improved by controlling the ratio of antigen molecule to QD—another way to improve the sensitivity of FOB. As aforementioned, the sensitivity of FOB can also be improved by increasing the quantum yield of QDs. If the state-of-the-art QDs could be employed with over 80% quantum yield, further enhancement of the sensitivity of the FOB would be a natural expectation.

Compared to conventional organic fluorophores, QDs have the potential to help achieving multi-targeting in a single fiber and simplify the performance of multiplexed analysis in FOB. To demonstrate the concept, we have employed four kinds of QDs emitting at 525 nm, 565 nm, 605 nm and 655 nm as labels to explore the possibility of the multiplexed assays in FOB. The emission spectra of the four kinds of QDs are shown in Fig. S5. Fib, HSA, HBs and IgG that were coupled to QDs showed maximal PL signals at 525 nm, 565 nm, 605 nm and 655 nm, respectively. A mixture of antigen attached to different color QD probes was used to detect antibody in the diluted samples. The signals of antigen-QDs conjugates that were linked to antibody immobilized on fiber core surface were detected. The photoluminescence spectra at different concentrations of the analytes are presented in Fig. 6, and the corresponding detailed results of the determination are given in Table S1. Although the multiplexed assay faces certain inherent shortcomings, such as antibody–antigen cross-reactivity, nonspecific interactions and background fluorescence, the as-prepared FOB for the simultaneous determination of analytes shows high

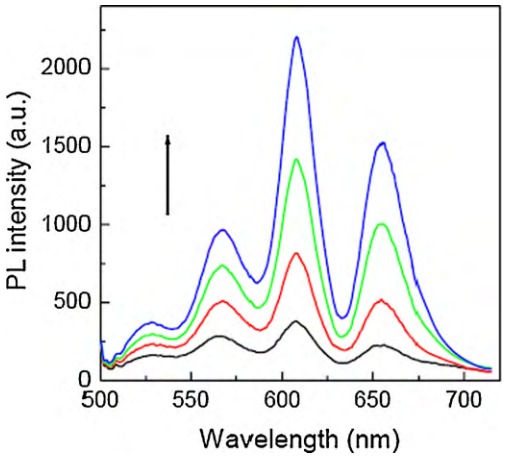

Fig. 6. Photoluminescence spectra of four kinds of complex of QD-labeled antigen and antibody in the fiber probe. Mix four kinds of antibody at different concentrations (50, 180, 380 and 600 ng/mL for each antibody), with a mixture of four kinds of antigen-QDs conjugates. The arrow presents the increase of concentration.

sensitivity and is suitable for fast quantitative determination of analytes. Here, the intervals of emission peaks for four kinds of QDs were chosen as 40 nm in order to avoid the overlapping of detection signal. In fact, more targets are possible by, e.g. reducing the intervals of emission peaks and using the software-deconvolution of composite spectra (Goldman et al., 2004).

4. Conclusions

This study is centered at constructing multi-targeting FOB using CdSe/ZnS core/shell QDs as labels for biodetection. It is concluded that the water-soluble CdSe/ZnS core/shell QD coated with amphiphilic polymers is an effective replacement of FITC. The detection limit of this approach is up to 5 ng/mL, lower than that of FITC (10 ng/mL). It is discussed that, on one hand, the size and mass of the QDs cause the interference with the human IgG mobility, resulting in the dropdown of the affinity and thus limiting the further improvement of the sensitivity of the FOB. On the other hand, the sensitivity of FOB can be improved by controlling the amount of IgG on the conjugates of QD-IgG or prolonging the time of detection. The most attractive potential of QDs is to enhance multi-analyte assay capabilities. We have demonstrated for the first time the realization of multiplexed assays in a single fiber of FOB using QDs as labels.

Acknowledgements

This work was supported by the program of the National Natural Science Foundation of China (60771051, 60601015, 10904142 and 60971026), the National High Technology Development Program (2006AA03Z335), and the exchange program between CAS of China and KNAW of the Netherlands.

Appendix A. Supplementary data

Supplementary data associated with this article can be found, in the online version, at doi:10.1016/j.bios.2010.05.032.

References

Abel, A.P., Weller, M.G., Duveneck, G.L., Ehrat, M., Widmer, H.M., 1996. Anal. Chem. 68, 2905–2912.
Alivisatos, P., 2004. Nat. Biotechnol. 22, 47–52.
Anderson, G.P., Jacoby, M.A., Ligler, F.S., King, K.D., 1997. Biosens. Bioelectron. 12, 329–336.
Chao, K.F., Zhang, Y.L., Kong, X.G., Zeng, Q.H., Liu, R.L., Wang, X., Feng, L.Y., Sun, Y.J., 2005. Proc. SPIE 6029, 6029221–6029227.
Dayal, S., Burda, C., 2007. J. Am. Chem. Soc. 129, 7977–7981.
Feng, L., Kong, X., Chao, K., Sun, Y., Zeng, Q., Zhang, Y., 2005. Mater. Chem. Phys. 93, 310–313.
Goldman, E.R., Anderson, G.P., Tran, P.T., Mattoussi, H., Charles, P.T., Mauro, J.M., 2002. Anal. Chem. 74, 841–847.
Goldman, E.R., Clapp, A.R., Anderson, G.P., Uyeda, H.T., Mauro, J.M., Medintz, I.L., Mattoussi, H., 2004. Anal. Chem. 76, 684–688.
Hines, M.A., Peters, R., Guyot-Sionnest, P., 1996. J. Phys. Chem. 100, 468–471.
Jaiswal, J.K., Simon, S.M., 2004. Trends Cell Biol. 14, 497–504.
King, K.D., Anderson, G.P., Bullock, K.E., Regina, M.J., Saaski, E.W., Ligler, F.S., 1999. Biosens. Bioelectron. 14, 163–170.
Leung, A., Shankar, P.M., Mutharasan, R., 2007. Sens. Actuators B 125, 688–703.
Mamedova, N.N., Kotov, N.A., Rogach, A.L., Studer, J., 2001. Nano Lett. 1, 281–286.
Mattoussi, H., Mauro, J.M., Goldman, E.R., Anderson, G.P., Sundar, V.C., Mikulec, F.V., Bawendi, M.G., 2000. J. Am. Chem. Soc. 122, 12142–12150.
Michalet, X., Pinaud, F.F., Bentolila, L.A., Tsay, J.M., Doose, S., Li, J.J., Sundaresan, G., Wu, A.M., Gambhir, S.S., Weiss, S., 2005. Science 307, 538–544.
Muller, C., Hitzmann, B., Schubert, F., Scheper, T., 1997. Sens. Actuators B 40, 71–77.
Myung, N., Bae, Y., Bard, A.J., 2003. Nano Lett. 3, 747–749.
O'Shannessy, D.J., BrighamBurke, M., Soneson, K.K., Hensley, P., Brooks, I., 1993. Anal. Biochem. 212, 457–468.
Peng, C., Li, Z., Zhu, Y., Chen, W., Yuan, Y., Liu, L., Li, Q., Xu, D., Qiao, R., Wang, L., Zhu, S., Jin, Z., Xu, C., 2009. Biosens. Bioelectron. 24, 3657–3662.
Pinaud, F., Kind, D., Moore, H., Weiss, S., 2004. J. Am. Chem. Soc. 126, 6115–6123.
Shan, G., Kong, X., Wang, X., Liu, Y., 2005. Surf. Sci. 582, 61–68.
Swift, J.L., Cramb, D.T., 2008. Biophys. J. 95, 865–876.
Taitt, C.R., Anderson, G.P., Ligler, F.S., 2005. Biosens. Bioelectron. 20, 2470–2487.
Wadkins, R.M., Golden, J.P., Ligler, F.S., 1995. Anal. Biochem. 232, 73–78.
Wang, M., Hou, W., Mi, C., Wang, W.X., Xu, Z.R., Teng, H.H., Mao, C.B., Xu, S.K., 2009. Anal. Chem. 81, 8783–8789.
Wang, Z.H., Jin, G., 2003. Anal. Chem. 75, 6119–6123.
Wu, X., Liu, H., Liu, J., Haley, K., Treadway, J., Larson, J., Ge, N., Peals, F., Bruchez, M., 2003. Nat. Biotechnol. 21, 41–46.
Yuan, J., Guo, W., Wang, E., 2008. Biosens. Bioelectron. 23, 1567–1571.
Zhao, K., Li, J., Wang, H., Zhuang, J., Yang, W., 2007. J. Phys. Chem. C 111, 5618–5621.